Computers in Biology and Medicine 109 (2019) 121–137

Contents lists available at ScienceDirect

Computers in Biology and Medicine

journal homepage: www.elsevier.com/locate/compbiomed

Modified fractional order IMC design based drug scheduling for cancer treatment

Nikhil Pachauri[a,*], Jyoti Yadav[b], Asha Rani[b], Vijander Singh[b]

[a] Electrical and Instrumentation Engineering, Thapar Institute of Engineering and Technology, Patiala, Punjab, 147004, India
[b] Instrumentation & Control Engineering Division, Azad Hind Fauz Marg, NSIT, Dwarka Sec-3, New Delhi, 110078, India

ARTICLE INFO

Keywords:
Chemotherapy
FOIMC
Modified FOIMC
Dragon fly algorithm

ABSTRACT

This paper aims to improve chemotherapy drug(s) scheduling of the drug dose injected into a patient. The existing practice has been established on experiments performed during the drug development process. In general, chemotherapeutic drugs are highly toxic in nature and directly affect the probability of a patient's survival. Therefore, a modified fractional order internal model control (MFOIMC) scheme with a minimal number of design parameters is proposed for effective drug scheduling. The proposed control scheme is a combination of fractional calculus and IMC. The fractional order IMC (FOIMC) is modified by incorporating an extra control loop with a proportional transfer function. Further, IPD and IMC control techniques are also designed for comparative analysis. The dragon fly algorithm (DA) is employed to optimize the parameters of the controller. Results show that the proposed control scheme provides a continuous and precise chemotherapeutic drug dose to the patient on a daily basis. It is also shown that MFOIMC improves IAE by 34% and 32% in comparison to IMC and FOIMC, respectively, which proves its superiority over other controllers.

1. Introduction

The word cancer refers to an uncontrolled growth of cells. These cells have the potential to penetrate neighbouring tissues and metastasize to other parts of the body [1]. A cancer or tumor enlargement in a patient's body is categorized into three phases: avascular, vasculature, and metastasis. Clinically, cancer is not declared until the tumor undergoes the metastasis phase in which the cells divide and transit to other parts of the body. The treatment of cancer is very critical in the metastasis phase because cancerous cells circulate in the whole body and form new tumors. According to a report by the Indian Council of Medical Research, approximately 1.43 million new cases of cancer were reported in India at the end of 2016, and this will reach around 1.75 million in 2020. Over 0.786 million deaths occurred in 2016 and this will rise to 0.88 million by 2020 [2]. These figures show that the number of cancer patients is increasing at an alarming rate. Therefore, researchers are focusing on effective treatment so that minimum harm is caused to normal body cells.

There are 5 major cancer treatment methods reported in the literature: chemotherapy, immunotherapy, hormone therapy, surgery and radiotherapy. Over the past years, chemotherapy has been frequently applied by clinicians. The goal of chemotherapy is to eradicate cancerous cells as much as possible or even eliminate them totally after the whole of the treatment period [3]. The process of killing cancerous cells depends upon the chemotherapeutic drug injected in the patient's body. It is a widely accepted fact that chemotherapeutic drugs are toxic in nature, which not only kill cancer cells but also destroy normal cells and hence directly endanger the life of the patient. Therefore it is important to select the appropriate dose which affects the cancerous cells with minimum damage to normal cells. The previous work on the optimum drug dose for chemotherapy is reviewed in Table 1.

The techniques discussed in Refs. [4–10] fail when there is any divergence of drug concentration and toxicity during the course of treatment. This is because no controller is used and the system acts as an open loop. Thus a closed loop system is required in cancer treatment to avoid this problem, as discussed in Refs. [11–16]. A closed loop chemotherapeutic drug delivery system comprises four main components: a sensor for measuring the concentration of the drug, a controller to evaluate the required drug dose, and a drug infusion pump to permit uninterrupted drug delivery to the patient. The transfer functions of the drug infusion pump and sensor are considered to be unity, and a mathematical model of the cancer patient is used [12]. Fig. 1 shows a schematic block diagram for the closed loop control of cancer chemotherapy.

Internal model control (IMC) and its variants have been successfully used for the control of various applications, such as continuous stirred

* Corresponding author.
E-mail addresses: nikhil.pachauri@thapar.edu (N. Pachauri), bmjyoti@gmail.com (J. Yadav), ashansit@gmail.com (A. Rani), vijaydee@gmail.com (V. Singh).

https://doi.org/10.1016/j.compbiomed.2019.04.013
Received 23 November 2018; Received in revised form 17 April 2019; Accepted 17 April 2019

Table 1
Literature survey for cancer chemotherapy.

Author's	Control strategies	Results obtained
Martin (1992–93) [4,5]	Numerical solution techniques based on analytical gradient	The size of tumor decreases rapidly during the treatment
Bojkov et al. (1993) [6]	Direct search algorithm (DSA) based on randomly chosen numbers and systematic search region contraction	DSA provides better drug schedule than analytical gradient numerical techniques
Tan et al. (2002) [7]	Distributed evolutionary computing (DEC) based on reserve elite individuals and migration interval	DEC is found better than simulated annealing and Tabu-search
Liang et al. (2006) [8]	Adaptive elitist population based genetic algorithm (AEGA)	Simulation results are identical to clinical trials
Tse et al. (2007) [9]	Iterative dynamic programming for multidrug chemotherapy	IDP gives better results than AEGA in terms of tumor reduction
Liang et al. (2008) [10]	Different toxicity terms are introduced in chemotherapy model and AEGA is used to solve it	Simulation results of improved model are found identical to clinical drug scheduling results
Algoul et al. (2011) [11]	IPD controller is designed and tuned using multi-objective genetic algorithm	99% reduction in cancerous cell is achieved from the initial volume
Alam et al. (2013) [12]	MOGA IPD controller is designed for cell cycle specific model	The reduction in proliferating cells is 72% in case of IPD controller which is higher than PID
Moradi et al. (2013) [13]	Three control strategies based on H_∞ controller, optimal linear regulator and nonlinear optimal controller are designed	H_∞ controller shows better performance in comparison to other control structures
Szeles et al. (2014) [14]	H_∞ control is proposed for control of tumor growth under angiogenic stimuli	H_∞ is more robust as compared to PID towards variations in tumor volume ranging from 5000 to 15000 mm^3
Khadraoui et al. (2016) [15]	2-DOF-PID is proposed for cancer chemotherapy	Number of cancerous cells at the end of treatment is 1 from the initial $2*10^{11}$ cells
Pandey et al. (2018) [16]	Optimal ISA PID for drug concentration control	Results show that CSA-ISAPID reduces the number of cancerous cells upto 99.9% from its initial value

tank reactors, integrated processes, uncertain heavy duty vehicles, load disturbance rejection, heat flow experiments, etc. [17–21]. The advantage of incorporating IMC into PID and FOPID is that it decreases the number of parameters to be tuned in comparison to standard controllers. Various algorithms are used to tune the parameters of a controller in engineering applications. In the previous literature, genetic algorithms are what have mainly been used for controller tuning in chemotherapy [11,12]. Mirjalily proposed a new swarm intelligence based search algorithm, the dragon fly algorithm (DA) [22]. It has been applied to some standard applications and has demonstrated its ability to deal with complex problems. DA is used in different engineering problems, such as MPPT control, zero energy building design, generation dispatch of solar thermal systems [23–26], etc.

In chemotherapy the drug injection needs to be optimized so as to control its concentration at the site of the tumor and eradicate cancerous cells. It can be seen from the literature that mainly a PID controller is used for drug scheduling during cancer treatment. A one degree of freedom (DOF) PID control structure as used previously for drug scheduling [11,12,15], has one closed loop and cannot handle contradictory issues simultaneously. A 2-DOF control structure addresses simultaneously conflicting objectives, *e.g.* set-point tracking and parametric uncertainty [27–30,52]. This is due to the addition of an extra control loop with proportional gain which increases the overall gain of the system and improves the performance of the controller. MFOIMC has a 2-DOF control structure, *i.e.* two closed loops which regulate individually and lead to an efficacious control. However, the design and implementation of a fractional order IMC (FOIMC) for the precise control of drug scheduling in cancer chemotherapy still needs to be explored. Therefore, the objective of this work is to design a novel and efficient control scheme for controlling the concentration of a drug, which will be simple in structure and have a minimal number of parameters to be tuned. Hence an initial attempt is made in this article to design and implement a modified fractional order IMC (MFOIMC) for precise control of drug scheduling in cancer chemotherapy. DA is used to optimize the parameters of the proposed controller. The main steps of this are:

1. A Modified FOIMC (MFOIMC) controller is proposed for drug scheduling in cancer chemotherapy. The modification introduces an extra control loop with a proportional transfer function.
2. The parameters of the proposed controller are optimized using DA, and its performance is compared with a genetic algorithm, simulated annealing, particle swarm optimization and the krill herd algorithm.
3. The performance of the proposed controller is compared with FOIMC, I-PD [11,12] and the conventional IMC controller.
4. The robustness and sensitivity of the designed controllers to uncertainties in the parameters of the chemotherapy model are examined.
5. The performance of the proposed controller is tested on two cancer patient models.

The rest of this paper is organized as follows: in Section 2, the mathematical modelling of cell cyclic cancer patient model is discussed. Section 3 describes the control strategies. Optimization techniques are elucidated in Section 4. Simulation results, a discussion, and the conclusions of this research are given in Sections 5, 6, and 7 respectively.

2. Mathematical model

Recent research on cancer therapy focuses on new treatment methods, including targeted therapy [31] and patient tailored therapeutic intervention [32]. Tumor multiplicity and resistance towards cancer drugs are the main hurdles to accomplish clinical impression of these methods [33,34]. If the dose of the chemotherapeutic drug injected is low, no structured treatment interruption is necessary to

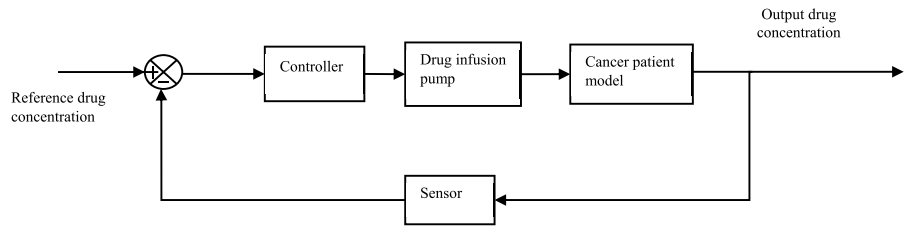

Fig. 1. Closed loop control of cancer chemotherapy.

restrict its side effects and toxicity level in the patient's body. However, for a high initial dose, it is required to interrupt the drug injection, which may lead to a rebound in the malignant cell population and directly risk the patient's life. Thus, the selection of the initial dose is a challenging task. Further, it is an immoral and risky process to examine all feasible combinations of drugs and schedules during clinical studies: thus, very few experiments are allowed on a patient. Mathematical models of cancer cells are an alternative to clinical experimentation. A mathematical model builds the relations between the drug dose, the tumor cells, and the normal cells. It facilitates testing hundreds of possible drug injection strategies as well as drug schedules and the best one may be chosen, which increases the probability of patient survival [35,36]. Several authors have proposed various mathematical models for cancer chemotherapy [37,38]. The actions of chemotherapeutic treatments are established on the mechanisms of cell cycle. Two types of mathematical models, *viz.* cell cycle nonspecific and cell cycle specific models, have been proposed on the basis of the cell cycle mechanism [3,4]. In the first type of model, the cell cycle is considered as unvarying and all tumor cells are considered to be same, so that the effect of the chemotherapeutic agents is the same on all tumor cells. In the second model it is assumed that different types of tumor cells exist, which are differently affected by the chemotherapeutic agents. This model is also known as a two-compartment model [3] and is shown in Fig. 2.

In the present work, a two-compartment cell cycle specific model [4] is considered to analyse the effects of chemotherapy on tumor growth. The mathematical model also demonstrates the effects of cytotoxic drugs on the normal cells along with malignant cells. The mathematical model under consideration is linear, described using first order linear differential equations. This restricts the mathematical representation to either exponential growth or decay without intermediate equilibrium. However, this is an acceptable attempt since an effective chemotherapeutic routine will inhibit the tumor growth close to its carrying capacity. Thus any nonlinearity such as logistic or Gompertz growth will be negligible, which permits the use of simpler model [3,51]. The model consists of three categories of cells: proliferating (P), quiescent (Q) and dead cells. A P cell has four phases in its cell cycle (G, S, G_2 and M) and Q cells have the G_0 stage [12]. The number of P and Q cells at the malignant sites are assumed to be 10^{12} and 10^9 respectively at the time of diagnosis. In the two-compartment model, 80% of the cell population are presumed to be Q cells and the remaining 20% are P cells (Dua et al. [3]).

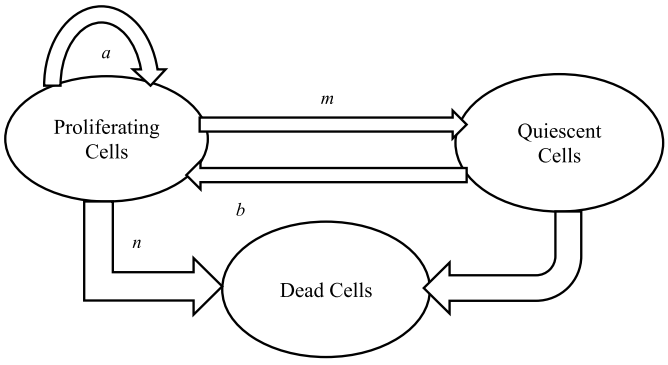

Fig. 2. Two-compartment cancer cell functional model.

The rates of change of P, Q and normal (Y) cells during the course of treatment are as follows:

$$\frac{dP}{dt} = (a - m - n)P(t) + bQ(t) - g(t)P(t) \tag{1}$$

$$\frac{dQ}{dt} = mP(t) - bQ(t),\ Q(0) = Q_0 \tag{2}$$

$$\frac{dY}{dt} = \alpha Y(t)\left(1 - \frac{Y(t)}{K}\right) - g(t)Y(t),\ Y(0) = Y_0 \tag{3}$$

where $g(t)$ is the rate of cancerous cell killing per unit of drug. The rate of change of drug concentration (D) and toxicity (T) are described by Equations (4) and (6) respectively, whereas the maximum allowable drug concentration and toxicity during the course of treatment are given by Equations (5) and (7) respectively.

$$\frac{dD}{dt} = u(t) - \beta D(t),\ D(t) = D_0 \tag{4}$$

$$10 \le D(t) \le 50 \tag{5}$$

$$\frac{dT}{dt} = D(t) - \mu T(t),\ T(t) = T_0 \tag{6}$$

$$T(t) \le 100 \tag{7}$$

The relation between the rate of cell killing and drug concentration is given by

$$g(t) = s_1 D(t) \tag{8}$$

where S_1 is a constant which relates the cell killing to drug concentration. In order to limit the toxic effect of the drug, the number of normal cells must be maintained within certain limits during the treatment.

$$Y_{min} \le Y(t) \le K,\quad for\ all\ t \in [0, T] \tag{9}$$

This mathematical model was simulated on an Intel® Core™ i5 CPU with 2.4 GHz frequency, 4 GB RAM in MATLAB. The description of the fundamental model parameters and nominal operating values have been taken from Refs. [3,12,51] and are given in Table 2. The simulated model was used to develop control strategies to estimate optimum drug scheduling for cancer treatment. Any drug scheduling process can be

Table 2
The fundamental model parameters [12].

Parameters	Description	Values
a	Rate of growth of P cells	0.5 day^{-1}
m	Mutation rate of P cells to Q cells	0.218 day^{-1}
n	The natural end of cycling cells	0.477 day^{-1}
b	Mutation rate of Q cells to P cells	0.05 day^{-1}
α	The rate of normal cell growth	0.1 day^{-1}
K	The carrying capacity of normal cell	10^9 cells
P	The proliferating cells population	$2*10^{11}$
Q	The quiescent cells population	$8*10^{11}$
Y	The normal cell population	10^9
Y_{MIN}	The limitation of normal cell	10^8

tested on a mathematical model of a cancer patient. This inspires control engineers to estimate the effect of a new algorithm for drug scheduling without applying it to an actual patient under treatment. The proposed control scheme is described in the subsequent section.

3. Control strategy

The objective of the present work is to achieve and then maintain the concentration of the drug at the site of the tumor close to the value of a set point. A new control strategy, which is a combination of fractional calculus and internal model control (FOIMC) will be proposed and then modified, leading to the Modified FOIMC (MFOIMC), for the optimal drug scheduling in cancer chemotherapy. The fractional calculus can model both short- and long haul memory. Fractional calculus originated due to progress in the field of regular calculus. The prime reference to this is associated with Leibniz and L'Hôpital in 1695, when the half-derivative was discussed. Fractional calculus is a generalization of integer-order integration and differentiation to fractional order (FO) integration and differentiation:

$$ {}_{\alpha}D_t^b = \begin{cases} d^b/dt^b & \Re(b) > 0 \\ 1 & \Re(b) = 0 \\ \int_{\alpha}^{t} (dt)^{-b} & \Re(b) < 0 \end{cases} \tag{10} $$

where α and t are the limits of operation and b is the fractional order. There are several definitions available in the literature, but the main ones used are that discussed by Grunwald-Letnikov (GL) and the so-called Riemann-Liouville (RL) definition. The GL definition is given as follows.

$$ {}_{\alpha}D_t^b f(t) = \lim_{r\to 0} r^{-b} \sum_{i=0}^{[t-\alpha/r]} (-1)^i \binom{b}{i} f(t-ir) \tag{11} $$

In this article, an FO differ-integral is realized using *Oustaloup's approximation*. This uses a filter of order $2N + 1$ which fits within a specified frequency range $[\nu_L, \nu_H]$. The final estimated transfer function corresponds to the fractional operator s^b where b is fractional power of s [39],

$$ s^b = G \prod_{m=-N}^{N} \frac{(s + \nu_{z_m})}{(s + \nu_{p_m})} \tag{12} $$

where G is the gain, $\nu_{z,m}$ and $\nu_{p,m}$ are the frequencies of the zeros and poles, respectively, of the filter, and represented as follows.

$$ \nu_{z_m} = \nu_L \left(\frac{\nu_H}{\nu_L}\right)^{\frac{m+N+(1/2)(1-b)}{2N+1}} \tag{13} $$

$$ \nu_{p_m} = \nu_L \left(\frac{\nu_H}{\nu_L}\right)^{\frac{m+N+(1/2)(1+b)}{2N+1}} \tag{14} $$

3.1. Fractional order internal model control

A block diagram representation of a closed loop control system based on the fractional order internal model control (FOIMC) is shown in Fig. 3. $G_m(s)$ is the internal plant model, $C_{FOIMC}(s)$ denotes the controller obtained by taking the inverse of $G_m(s)$, $G(s)$ is the actual plant, $D(s)$ is the external disturbance input and $C_{fc}(s)$ is the feedback controller.

The output equation from above block diagram is

$$ Y(s) = \frac{G(s)C_{FOIMC}(s)}{1 + C_{FOIMC}(s)[G(s) - G_m(s)]}R(s) \pm \frac{[1 - C_{FOIMC}(s)G_m(s)]}{1 + C_{FOIMC}(s)[G(s) - G_m(s)]}D(s) \tag{15} $$

In the literature there have been adopted different methods to design fractional order IMC controllers. In Ref. [40] there is designed an FO IMC PID in which the order of the filter is fractional and the plant is realized as a conventional integer order model. However, the fractional IMC PIDs in Refs. [39,42–44] and the fractional 2-DOF IMC-PID in Ref. [45] are designed using an FO plant model. In the present work, the cancer patient model is approximated as a fractional order plant model using the impulse response invariant discretization method in the time domain [46]. The steps followed in the design of the FOIMC controller are the same as those for a conventional IMC [39].

Step 1. The first step is to estimate the plant as FO plant model (Fig. 4).

$$ G_m(s) = \frac{K}{Ts^{\mu} + 1} \tag{16} $$

Step 2: Factor the FO plant model into invertible and noninvertible parts:

$$ G_m(s) = G_m^+(s) * G_m^-(s) \tag{17} $$

where the invertible part $G_m^-(s) = \frac{K}{Ts^{\mu}+1}$ and the noninvertible part is $G_m^+(s) = 1$

Step 3: The controller $C_{FOIMC}(s)$ is evaluated as follows:

$$ C_{FOIMC}(s) = \frac{1}{G_m^-(s)} F(s) \tag{18} $$

$$ F(s) = \frac{1}{(1 + \eta s)^n} \tag{19} $$

where $F(s)$ is the IMC filter with filter constant η, which can be selected in such a way that $C_{FOIMC}(s)$ is realizable. Substituting $F(s)$ in Equation (18) and taking the value of $n = 1$ to make the proper ratio yields

$$ C_{FOIMC}(s) = \frac{Ts^{\mu} + 1}{K} * \frac{1}{(1 + \eta s)} \tag{20} $$

The relation between $C_{FOIMC}(s)$ and the conventional feedback controller $C_{fc}(s)$ can be easily found:

$$ C_{fc}(s) = \frac{C_{FOIMC}(s)}{1 - C_{FOIMC}(s)G_m(s)} \tag{21} $$

The feedback controller $C_{fc}(s)$ contains both an internal FO plant model and the FOIMC controller. Thus Equation (15) can be rewritten as follows:

$$ Y(s) = \frac{G(s)C_{fc}(s)}{1 + C_{fc}(s)G(s)}R(s) \pm \frac{1}{1 + C_{fc}(s)G(s)}D(s) \tag{22} $$

3.2. The modified fractional order IMC

The standard FOIMC provides good performance as long as the value of the filter coefficient η is in the medium range. But if the value of η is low, FOIMC suffers from input saturation. Thus a decrease in η improves the disturbance rejection capability of FOIMC but at the same time the set-point tracking ability of controller deteriorates. It always produces a control signal greater than the maximum permissible dose and hence gets saturated, due to which the whole control system behaves like an open loop system. In order to curb this problem and improve the tracking and disturbance rejection, a modification is proposed in the control structure which leads to the modified FOIMC controller (MFOIMC) shown in Fig. 5. An extra feedback control loop is introduced in the structure with proportional controller $C_a(s) = K_{pa}$. The

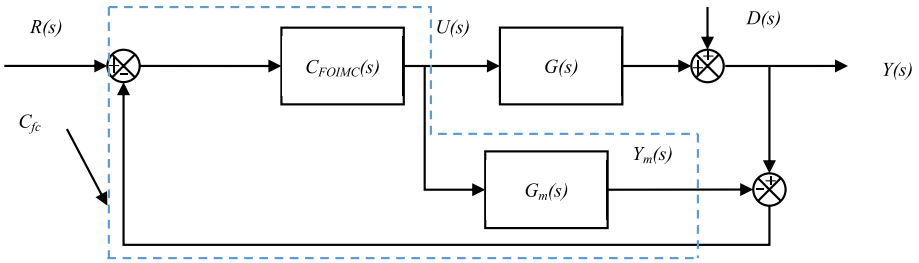

Fig. 3. Block diagram of FOIMC controller.

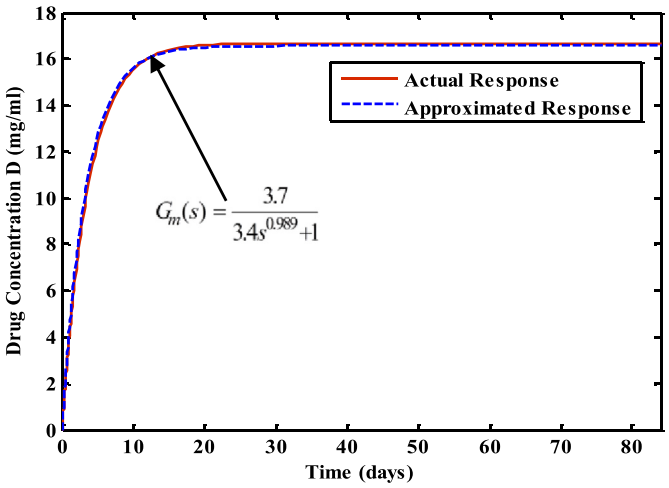

Fig. 4. Response of approximate FO plant model.

proposed structure is a 2-DOF IMC with two closed loops as discussed earlier. It is able to address both the contradictory issues: set point tracking and disturbance due to parametric uncertainty. The modified output equation can be written from Fig. 5 as

$$Y(s) = \frac{G(s)[C_{fc}(s) + C_a(s)]}{1 + [C_{fc}(s) + C_a(s)]G(s)}R(s) \pm \frac{1}{1 + [C_{fc}(s) + C_a(s)]G(s)}D(s) \quad (23)$$

It can be seen from Equations (22) and (23) that if the value of $C_a(s)$ is regulated appropriately to make $(C_{fc}(s) + C_a(s))*G(s) > > 1$, it effectively rejects disturbances occurring due to parametric uncertainties. It can also be deduced that K_{pa} not only enhances the overall gain of the system but also improves the tracking ability of the control structure. Further, when the output of FOIMC controller gets saturated, the controller $C_a(s)$ can compensate for those consequences. This in turn improves the tracking behaviour. The MFOIMC contains only two design parameters: the filter coefficient η and the gain K_{pa}. Thus both control loops complement each other and improve the overall performance of system. A detailed performance analysis of MFOIMC is given in Section 5.

4. Optimization of controller parameters

The foremost and essential prerequisite for effective execution of a control scheme is to evaluate the optimal values of the design parameters. Advances in the area of optimization techniques provide excellent solutions to controller tuning problems. Several optimization techniques are used for controller tuning in different applications. Optimization techniques are generally based on evolution and swarm intelligence. Genetic algorithm (GA), evolutionary strategy (ES), differential evolution algorithm (DE), genetic programming (GP), etc. are the evolution based techniques, whereas particle swarm optimization (PSO), ant lion colony optimization (ALO), etc., are swarm intelligence based techniques. Swarm intelligence has certain advantages over evolutionary algorithms:

- Flexibility is the main advantage of swarm intelligence algorithm due to which it is employed in various fields.
- Swarm intelligence uses fewer variables and operators than evolutionary algorithms do.
- Swarm intelligence techniques preserve the data of the search space, whereas evolutionary algorithms discard the previous generation's data.

As per the 'no free-lunch' theorem [47], a single optimization technique is not able to solve all optimization problems. Therefore, various new meta-heuristic algorithms have been proposed which verify the theorem. In this work, several optimization algorithms, *viz.*, GA, SA, PSO, KH and DA, have been tried in order to select the most suitable technique for optimum tuning of MFOIMC controller. The concept of the genetic algorithm (GA) is based on natural evolution as given by Darwin. It replicates the process of natural selection where the appropriate individuals are selected in order to produce offspring. The performance of a GA generally depends on its parametric settings but

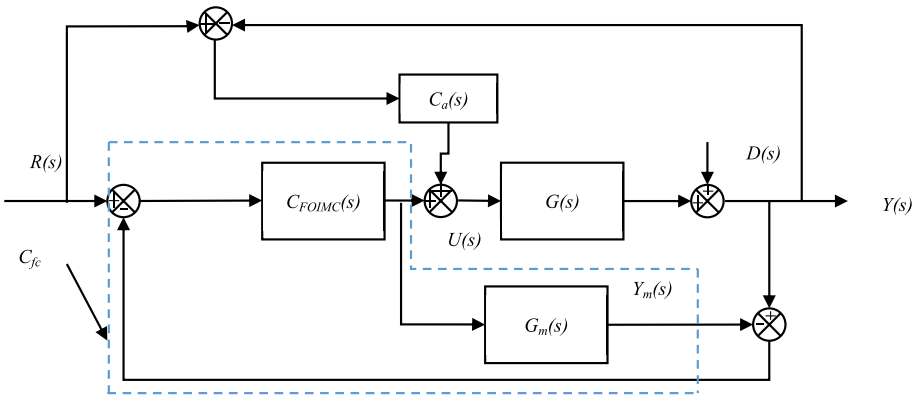

Fig. 5. Block diagram of MFOIMC.

Table 3
Governing parameters of DA.

DA parameter	Value
Number of design variables	2 (MFOIMC)
Population size	20
Maximum iteration	100
Parameter bounds for MFOIMC	η ε [1.06, 1.17], and K_{pa} ε [30, 60]

there is no generalized rule available in the literature for making these settings. As an illustration, several types of selection operators are available in the literature, which affect the performance of a GA. Simulated annealing (SA) is inspired by the process of annealing in metallurgy. Annealing involves the heating and cooling of a material to increase its size and reduce its defects. SA works by generating a test point in the vicinity of the current iterate and on the basis of the values of a certain function it decides whether the present point should be replaced by the test point or not. Convergence to an optimal solution can theoretically be assured only after an infinite number of iterations have occurred, controlled by a cooling schedule. An appropriate cooling schedule is needed in the finite-time implementation to simulate the asymptotic behaviour of SA. Because of this reason, SA suffers from sluggish convergence rate and it may stroll around the optimal solution.

Particle swarm optimization (PSO) is based on the swarming of bird flocks. It starts the optimization using randomly generated solutions, commonly known as artificial particles. Each particle in a swarm has an associated random velocity and acceleration. PSO suffers from numerous practical issues, *e.g.* the particle can deviate from its presently defined maximum velocity and acceleration constants. It is easy to implement as compared to GA and SA, but a rigorous analysis is required to select the initial weights, cognitive and social constants [48]. Krill herd (KH) is inspired by the swarming of Antarctic krill. One of the main characteristics of this species is its ability to form large swarms. The density of a krill swarm decreases in the presence of predators, such as seals, penguins or seabirds. A single krill is removed from the group when predators attack the krill swarm, which results in the development of new krill swarms with reduced populations. The herding of krill has two main goals: (1) increasing krill density, and (2) reaching food. Further selection of genetic operators and motion calculation are two important phases in KH. Its performance depends on the type of

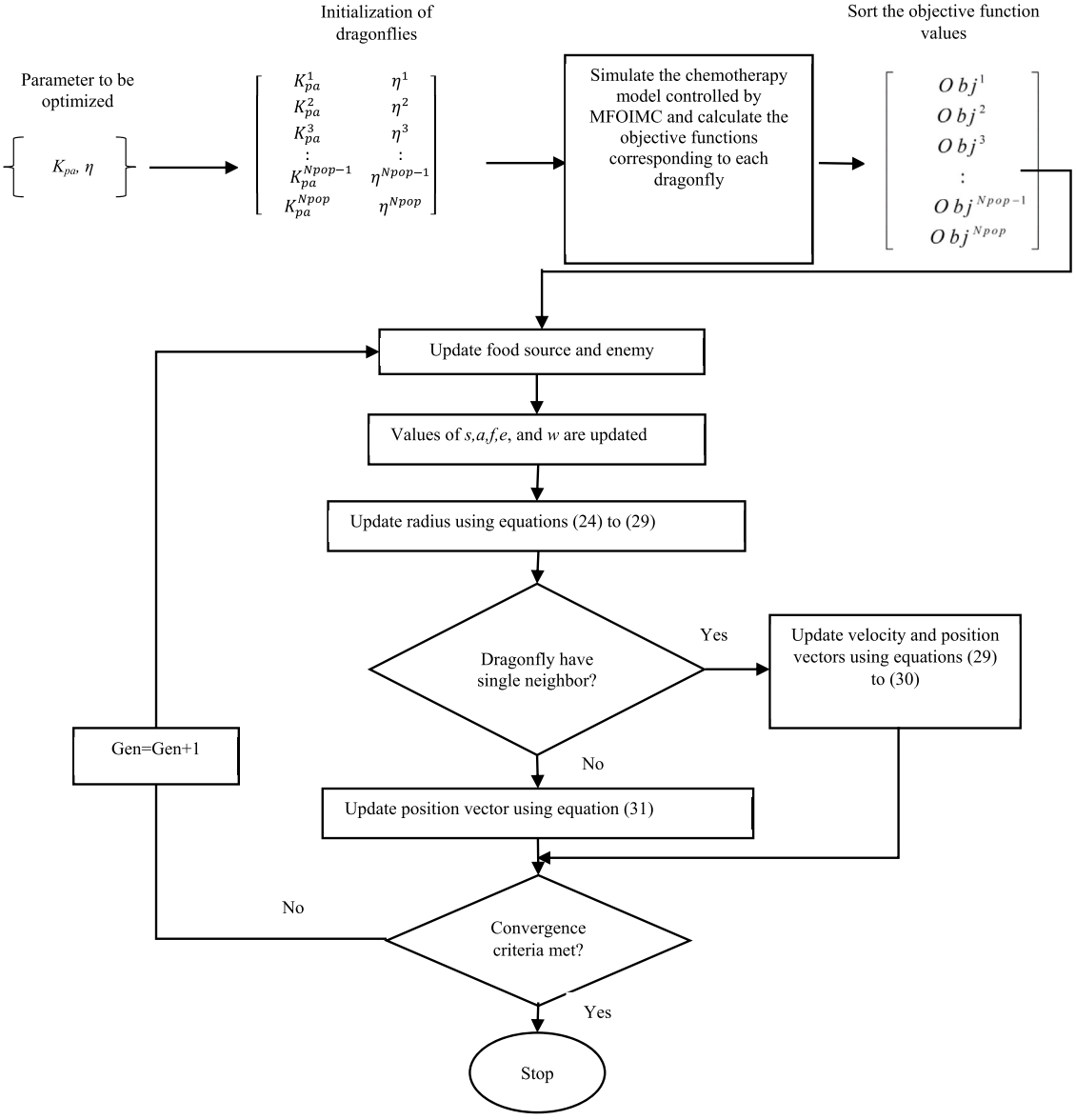

Fig. 6. Flowchart for DA-based tuning of MFOIMC controller.

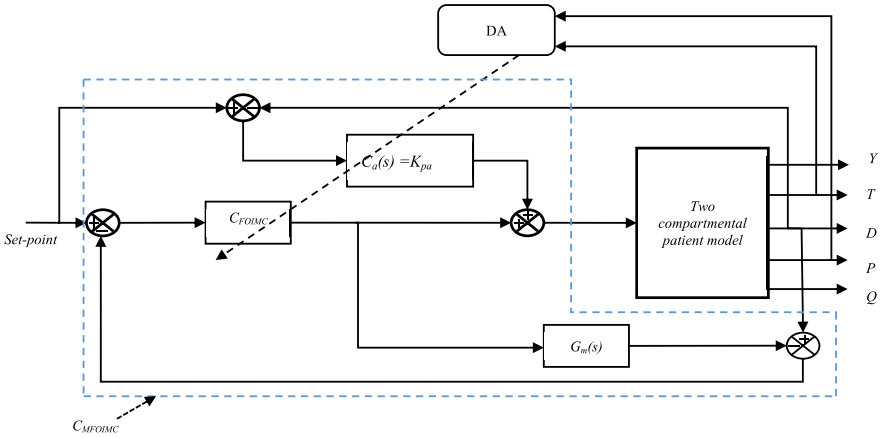

Fig. 7. Schematic diagram of DA-tuned MFOIMC based chemotherapeutic drug scheduling scheme.

Table 4
Constraints for optimization of controller parameters.

Notations	Description	Range
RC_P	% of reduction of P cells	$RC_P > 65\%$
RC_Q	% of reduction of Q cells	$RC_Q > 55\%$
$Y(t)$	No. of normal cells	$Y(t) > 1*10^8$
$T(t)$	Toxicity	$T(t) \leq 100$
$D(t)$	Drug concentration	$10 < D(t) \leq 50$

mutation, crossover and selection operators employed [49].

The dragonfly optimization algorithm (DA), a swarm intelligence based optimization technique proposed by Mirjalili [22], is also employed for optimizing the parameters of the proposed controller. The key benefit of DA in comparison to other famous meta-heuristic algorithms is that it doesn't need any particular set of input parameters. Moreover, it is direct and free from computational difficulty. The dragonfly is recognized as a minor slayer, which hunts nearly all smaller insects present in nature. Dragonflies have exceptional and unpredictable swarming behaviour during poaching and migration. The first type is known as a stationary (nourishing) swarm and the second is an active (migration) swarm. In a stationary swarm, dragonflies move in minor clusters to hunt rhopalocera and culicidae. The main features of the stationary swarm are indigenous schedules and rapid variations in flying route, whereas in an active swarm all dragonflies migrate in one direction to a place far away. The two categories of swarming correspond to the exploration and exploitation stages of optimization [23,47]. The swarming of dragonflies is best described in terms of separation, cohesion, alignment, attraction of food and defense from enemies.

Separation involves the avoidance of collisions between neighbouring individuals and is given by

$$S_i = -\sum_{j=1}^{N} (X - X_j) \tag{24}$$

S_i	separation of ith individual
X	position of current individual
X_j	position of jth neighbouring individual
N	number of neighbouring individuals

Alignment describes the matching of the velocities of the individuals in the neighbourhood

$$A_i = \frac{\sum_{j=1}^{N} (V_j)}{N} \tag{25}$$

A_i	alignment of ith individual
V_j	velocity of jth neighbouring individual.

Cohesion indicates the distance of an individual from the centre of mass of the other individuals.

$$C_i = \frac{\sum_{j=1}^{N} (X_j)}{N} - X \tag{26}$$

The existence of a swarm depends on attraction of food and interference from enemies, as given by Equations (27) and (28) respectively.

$$F_i = X^+ - X \tag{27}$$

$$E_i = X^- + X \tag{28}$$

F_i	food source of ith individual
E_i	position of enemy of ith individual
X^+	position of food source
X^-	position of enemy

The position (X) and step (ΔX) vectors are updated in Equations 29 and 30 so as to obtain the optimum solution.

$$\Delta X_{t+1} = (sS_i + aA_i + cC_i + fF_i + eE_i) + w\Delta X_t \tag{29}$$

s	separation weight
S_i	separation of ith individual
a	alignment weight
c	cohesion weight
C_i	cohesion of ith individual
f	food factor
e	enemy factor
w	inertia weight
t	iteration counter

$$X_{t+1} = X_t + \Delta X_{t+1} \tag{30}$$

The introduction of the concept of a Levy flight in Equation (31)

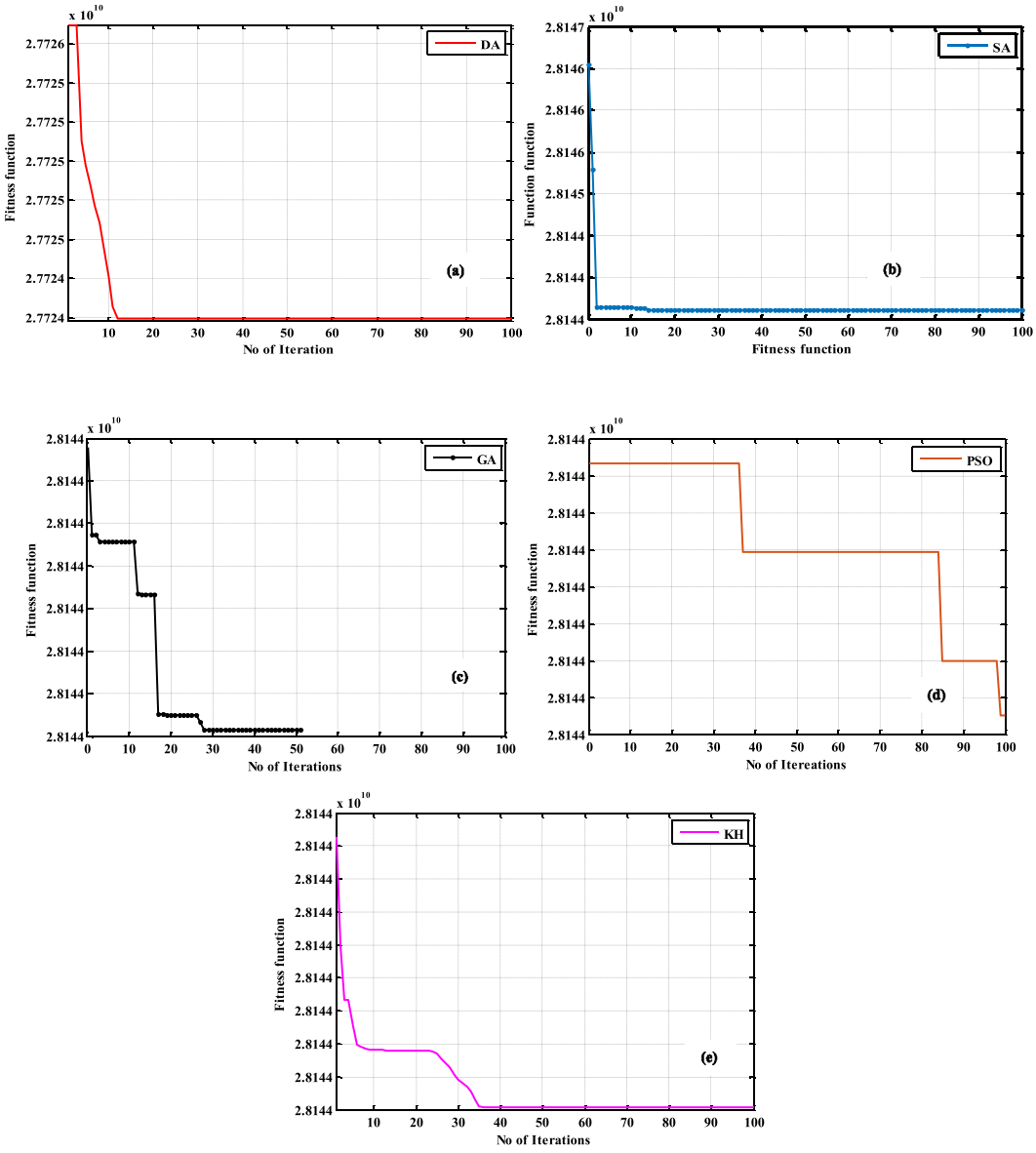

Fig. 8. Convergence of different optimization techniques for tuning MFOIMC. (a) Dragonfly (b) Simulated annealing (c) Genetic algorithm (d) Particle swarm (e) Krill herd.

Table 5
Optimized parameter values of MFOIMC with respective fitness values for different optimization algorithms.

Optimization techniques	K_{pa}	η	Fitness value
DA	55.02	1.110	$2.772460*10^{10}$
SA	48.10	1.100	$2.814359*10^{10}$
GA	48.12	1.081	$2.814382*10^{10}$
PSO	49.02	1.092	$2.814397*10^{10}$
KH	50.03	1.083	$2.814360*10^{10}$

[23] enhances the randomness of the behaviour and exploration time of the dragonflies.

$$X_{t+1} = X_t + Levy(d) \times X_t \quad (31)$$

t	iteration counter
d	dimension of position vector

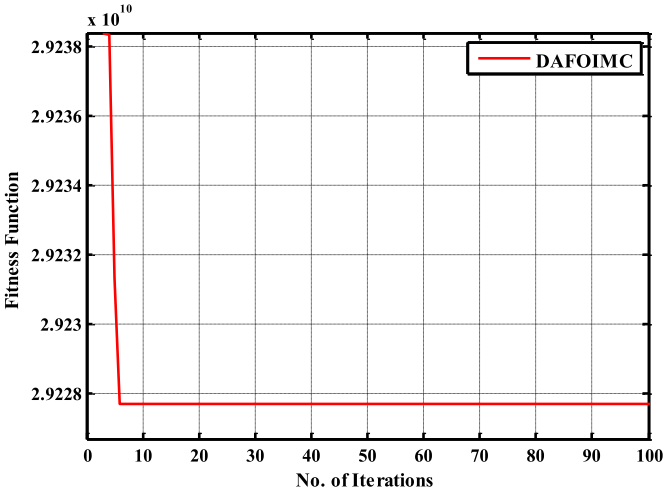

Fig. 9. Convergence plot for DA tuned FOIMC.

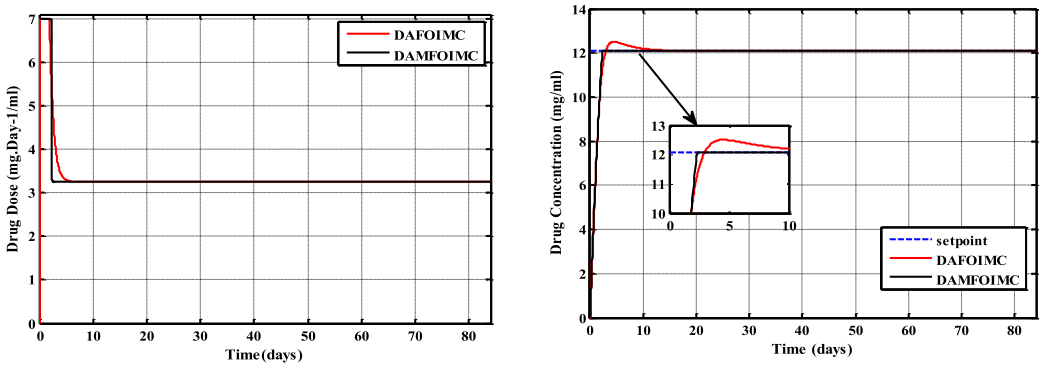

(a) Drug dose (b) Drug Concentration at tumor site

Fig. 10. Drug concentration control for $S_1 = 12.08$ using DAFOIMC and DAMFOIMC.

Table 6
Quantitative analysis of DAFOIMC and DAMFOIMC for $S_1 = 12.08$

Controllers	%Os	Settling time (days)	Rise Time (days)
DAFOIMC	3.5046	7.3769	1.9540
DAMFOIMC	0.0167	2.2595	1.8370

Table 7
Performance measures of DAMFOIMC chemotherapeutic drug scheduling scheme.

Controllers	Reduction in P cells	Reduction in Q cells	Toxicity T	Remaining Y cells
DAFOIMC	72.17%	60.32%	31.12	1.0057*10^8
DAMFOIMC	72.40%	60.50%	30.43	1.0092*10^8

The Levy flight distribution is given by

$$Levy(d) = 0.01 \times \frac{r_1 \times \sigma}{|r_2|^{1/\beta}} \tag{32}$$

where r_1 and r_2 are random numbers, β is a constant, and σ is given by

$$\sigma = \left(\frac{\Gamma(1+\beta) \times \sin\left(\frac{\pi\beta}{2}\right)}{\Gamma\left(\frac{1+\beta}{2}\right) \times \beta \times 2^{\left(\frac{\beta-1}{2}\right)}} \right) \tag{33}$$

The governing parameters of DA and a detailed flowchart of the DA-tuned MFOIMC for the chemotherapy model are given in Table 3 and Fig. 6 respectively.

5. Simulation results

In this work, an MFOIMC-based chemotherapy drug scheduling scheme is proposed to maintain the drug concentration at its desired level. An FO controller is designed using a fifth-order Oustaloup filter approximation with frequency range $[10^{-3}, 10^{-2}]$ rad/s. For fair comparison the design parameters of the MFOIMC and FOIMC are tuned with the help of a DA, which leads to DA-MFOIMC and DA-FOIMC.

5.1. Case study 1

A schematic diagram of the chemotherapeutic drug scheduling scheme based on a DA-tuned MFOIMC is shown in Fig. 7. A two-compartment cancer cell functional model is employed for the experimentation. The optimization of the controller parameters requires the selection of an appropriate objective function that is to be minimized or maximized. In this work a weighted sum of the number of proliferating cells $P(t)$ and the average toxicity $T(t)$ is considered as the objective function for the treatment process, as given by Equation (34).

$$J_1 = w_1 \times P(t_f) + w_2 \times \left(\frac{1}{t_f} \int_0^{t_f} T(t)dt \right) \tag{34}$$

Here, w_1 and w_2 are weights allotted in an optimum manner according to the requirements of the system. The combination of these weights should satisfy the constraint [39,40].

$$\sum_{j=1}^{n} w_j = 1 \tag{35}$$

where n denotes the number of design specifications. In the present paper, w_1 and w_2 are set to 0.50. The constraints considered in the optimization of the proposed controller are given in Table 4.

The tuning of the controller is a combinatorial problem and accuracy is an important attribute; therefore the optimization of the controller parameters is required for the efficient performance of the plant under study. As discussed previously, the GA, SA, PSO, KH and DA optimization algorithms have been tested for tuning the controller parameters of the MFOIMC. The most suitable algorithm has been selected by comparing their performance while taking common parameters such as the lower bound and upper bound of the tuning parameters, population size, stopping criteria and objective function to be same. The convergence curves of the different optimization techniques shown in Fig. 8 reveal that GA converges prematurely. A possible reason may be the poor parametric settings of the GA and there is no general rule available in the literature for this purpose. In the case of PSO (Fig. 8 (d)) the optimal region is not explored before the fulfillment of the specified stopping criterion. SA (Fig. 8 (b)) gives better results than GA and PSO, but the selection of an appropriate cooling schedule for SA is a cumbersome task. On the other hand, DA (Fig. 8 (a)) succeeds in finding the optimal region and is computationally economical as it takes only 11 iterations, *i.e.* 220 function evaluations, to get the optimal solution. Apart from this, DA offers a high convergence rate with appreciable accuracy in comparison to KH. Table 5 shows an analytical comparison of the considered optimization algorithms on the basis of their fitness values. It is clearly seen that DA outperforms the other algorithms as its fitness value is less. Hence it can be deduced that DA is the most suitable optimization technique in comparison to the other algorithms for the current application. Thus DA has been selected to optimize the parameters of the designed controllers. Fig. 9 shows the convergence plot for the DA-tuned FOIMC controller.

Initially no drug dose is infused to the patient and the difference between the set-point and the actual output $D(t)$ is a maximum. As the course of treatment progresses, the error decreases and reduces to zero at the end of treatment. In order to make the chemotherapeutic treatment efficient, the drug concentration must be maintained at the defined level. This is achieved by employing a fixed level of signal, known

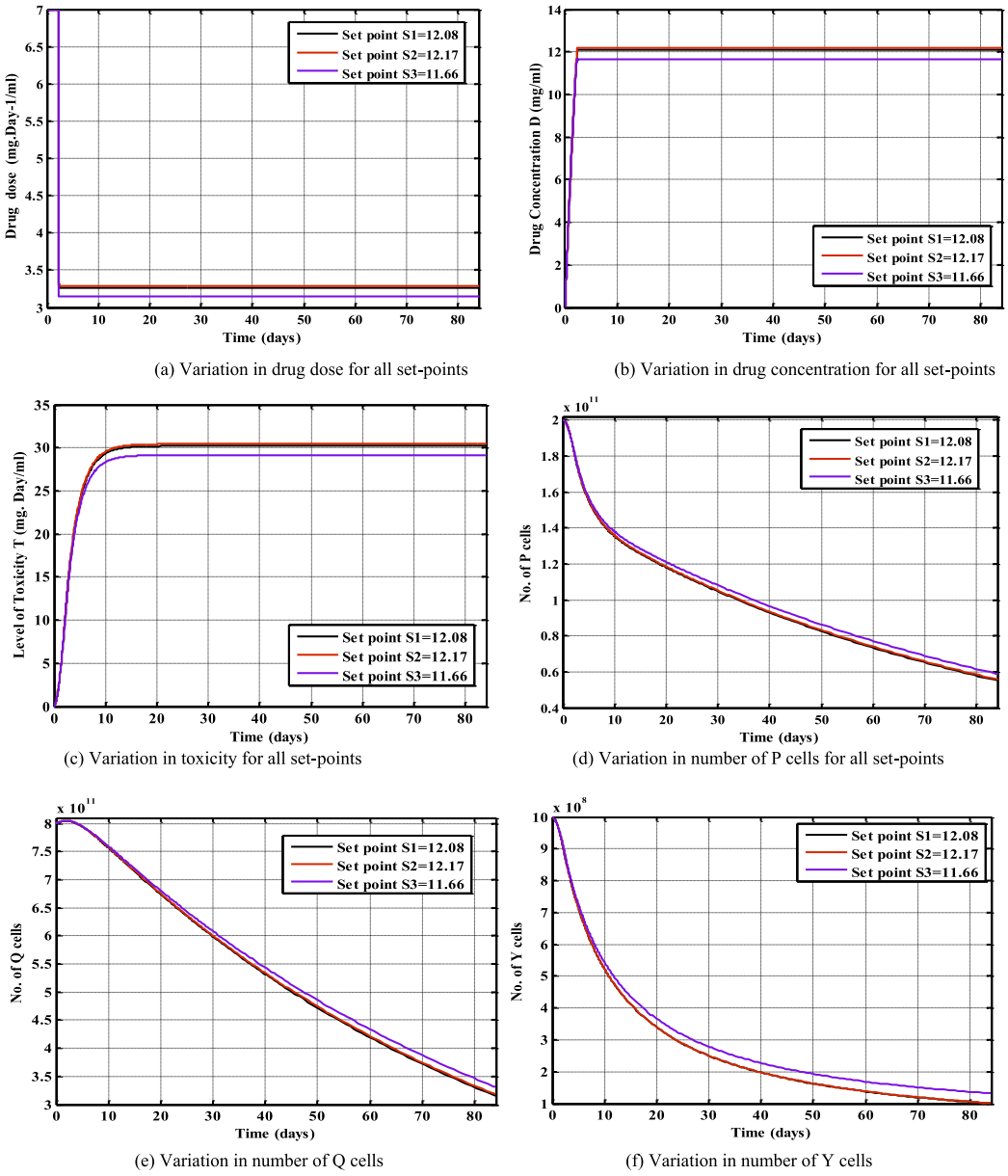

(a) Variation in drug dose for all set-points

(b) Variation in drug concentration for all set-points

(c) Variation in toxicity for all set-points

(d) Variation in number of P cells for all set-points

(e) Variation in number of Q cells

(f) Variation in number of Y cells

Fig. 11. Performance analysis of DAMFOIMC for different set-points.

Table 8
Performance measures of DAMFOIMC chemotherapeutic drug scheduling scheme under different set points.

Controllers	Set-points	Reduction in P cells	Reduction in Q cells	Number of Y cells remaining	Maximum toxicity
DAMFOIMC	$S_1 = 12.08$	72.4%	60.6%	$1.0044*10^8$	30.2
	$S_2 = 12.17$	72.1%	60.2%	$1.0089*10^8$	30.4
	$S_3 = 11.66$	70.5%	58.6%	$1.3214*10^8$	29.1

as a step input. In this work, three set-points, $S_1 = 12.08$, $S_2 = 12.17$, and $S_3 = 11.66$, are considered for drug concentration [12]. The designed controllers DAMFOIMC and DAFOIMC are tuned for set-point $S_1 = 12.08$. Once a controller is tuned it does not require retuning for changes in the set-point. Examining the controller for an altered set-points establishes the ability of the controller to handle uncertainties in the process. A performance comparison of DAMFOIMC and DAFOIMC for the set-point $S_1 = 12.08$ is shown in Fig. 10 and a quantitative analysis is given in Table 6. The results demonstrate the efficacy of the proposed DAMFOIMC. It is evident from the results that the incorporation of the extra control loop reduces considerably the overshoot, settling time, and rise time as compared to DAFOIMC. Thus the proposed controller successfully handles the situation of tight drug concentration control in cancer chemotherapy as compared to DAFOIMC. Similarly, DAMFOIMC outperforms DAFOIMC for the other set-points also.

It can be seen from Table 6 that the drug concentration settles down within 2.2595 days with an overshoot of 0.0167% for DAMFOIMC, whereas DAFOIMC takes 7.3769 days with an overshoot of 3.5046%. This demonstrates the good transient performance as well as the good steady state performance of the proposed controller. The goal of the controller is to maintain the drug concentration at the desired set-point.

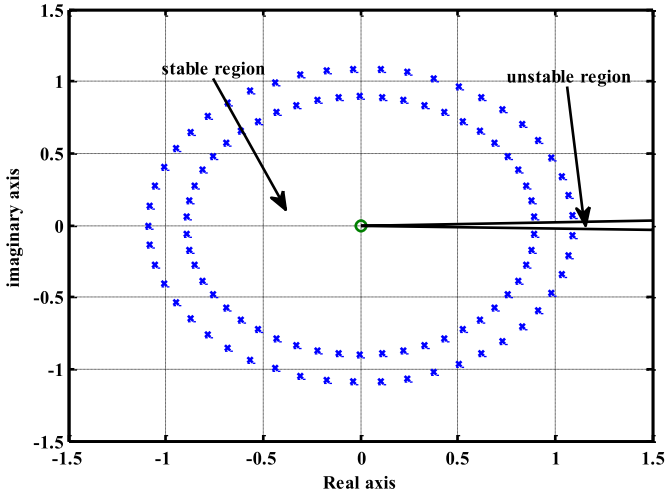

Fig. 12. Stability region of closed loop chemotherapy drug scheduling system.

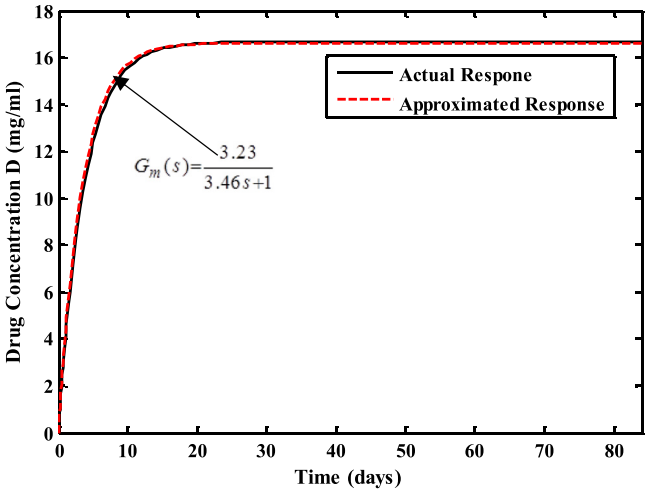

Fig. 13. Approximate IO plant model response.

The chemotherapeutic drug is also responsible for the reduction in the number of P and Q cells, so that the P cells cannot infiltrate into the other regions of the body. Besides killing cancerous cells, the drug also reduces the number of normal cells as a side effect. Hence the toxic effect of the drug is inversely proportional to the reduction in the number of normal cells. The remaining normal cells indicate the physiological state of the patient at the end of the chemotherapy. Performance indices of DAMFOIMC and DAFOIMC chemotherapeutic drug scheduling schemes for $S_1 = 12.08$ are shown in Table 7.

It can be seen from the table that for the same set-point, the percentage reduction in the number of P cells and Q cells with DAFOIMC is 72.17% and 60.32% respectively, which is lower than for DAMFOIMC. The value of toxicity observed with DAFOIMC is 31.12, whereas DAMFOIMC has a lower toxicity: 30.4. The objective of reducing the P and Q cell population with a minimum toxicity level is thus achieved using the proposed control scheme. As discussed, the toxicity of the chemotherapeutic drug also affects the population of normal cells. With DAMFOIMC, the population of Y cells is larger than for DAFOIMC, and thus the patient is in a better state. Fig. 11 displays the action of DAMFOIMC for all the set-points. Performance measures for DAMFOIMC for different set-points are given in Table 8.

It can be seen from Fig. 11 (a) that a high dose of the drug is given to the patient at the start of treatment. It settles down to its minimum value within 2.5 days for the remaining course of treatment. The maximum value is the same for all the set-points but there are differences in the minimum values. The minimum values at which drug doses settle down for S_1, S_2, and S_3 are 3.261, 3.2856 and 3.1470 mg Day^{-1}/ml respectively. Fig. 11 (b) shows the drug concentrations for S_1, S_2, and S_3 at the malignant tumor site. It is important to note that for all cases the drug concentration increases in the same manner to the reference levels.

The level of toxicity increases initially and settles to its final value as shown in Fig. 11 (c). The maximum values of toxicity for the set-points are shown in Table 8. The level of toxicity for all the cases is under control and less than the prescribed value (Equation (7)). Similarly, a reduction in the number of P and Q cells is visible in Fig. 11 (d) and (e). This reduction starts from the maximum value and reaches the minimum value after 84 days of treatment. The chemotherapeutic drug untowardly affects the population of normal cells (Y cells). The number of Y cells considered before chemotherapy for this work is 10^{11}. Fig. 11(f) demonstrate the variations in the number of Y cells for the whole course of treatment. The number of Y cells remaining after 84 days is given in Table 8 for each of the set-points.

Stability is one of the important aspects in a closed-loop system. If the output of the system is infinite for a finite input, the closed-loop system is said to be unstable. According to *Matignon's stability theorem* [50], an FO closed loop system is stable if the argument $K = 1$, and the commensurate-order q is in the range (0, 1). Fig. 12 shows the locus of all roots of the closed loop in the complex plane, with the stable and unstable regions, for the chemotherapy drug scheduling system. The value of the argument $K = 1$ and the order $q = 0.02$, which indicates that the system is stable.

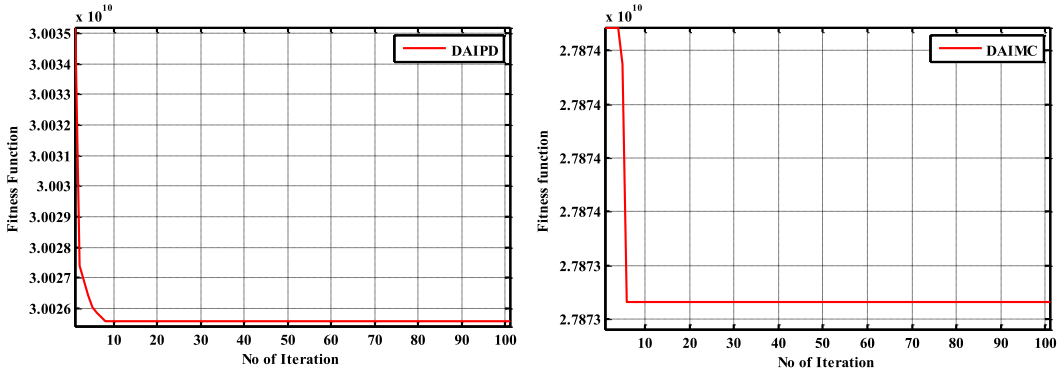

(a) Convergence graph of DA tuned IPD (b) Convergence graph of DA tuned IMC

Fig. 14. (a) Convergence graph of DA tuned IPD (b) Convergence graph of DA tuned IMC.

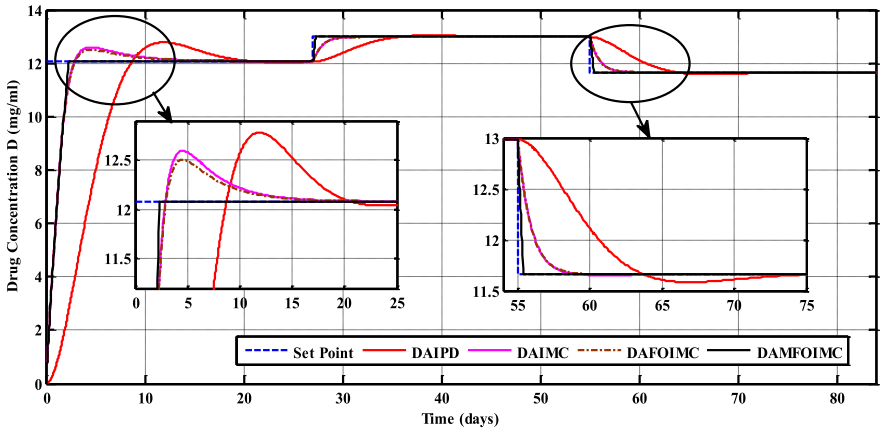

(a) Drug concentration D

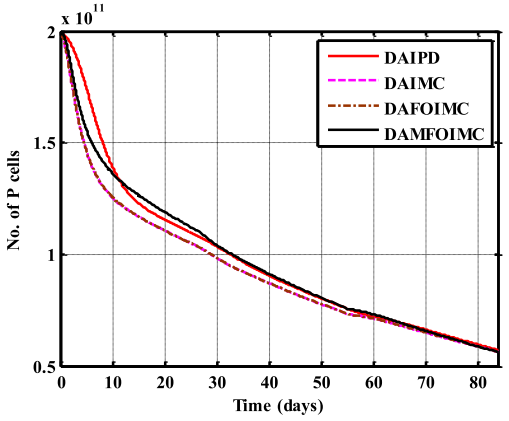

(b) Reduction in P cells

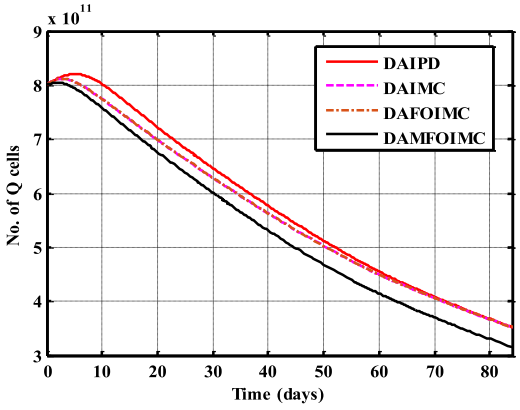

(c) Reduction in Q cells

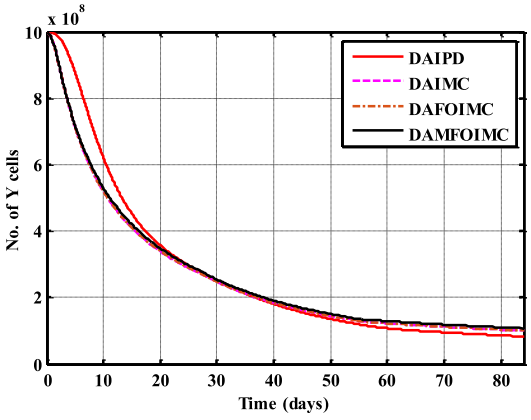

(d) Variation in Y cells

Fig. 15. Set-point tracking comparison for designed controllers.

Table 9
Quantitative analysis of set-point tracking for designed controllers.

Controllers	ISE	IAE	Average Toxicity (T_{avg})
DAIPD	434.50	64.39	37.154
DAIMC	98.78	17.71	34.170
DAFOIMC	98.57	17.30	34.145
DAMFOIMC	96.42	13.13	32.451

5.2. Comparative analysis

In the present work DA tuned IPD [11,12] (DAIPD) and DA tuned integer order internal model controller (DAIMC) have also been designed in order to justify the effectiveness of the proposed DAMFOIMC controller. The design procedure of the IMC is same as that of the FOIMC controller except for the integer order (IO) approximate plant model (Fig. 13) using the impulse response discretization method.

The IMC controller transfer function with filter coefficient α is

$$C_{IMC} = \frac{(1 + 3.46s)}{3.23\alpha s} \tag{36}$$

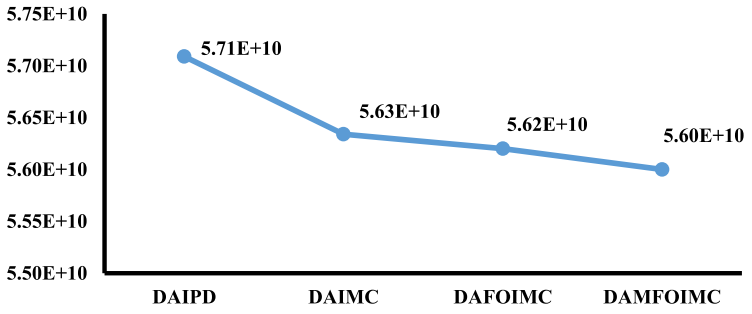

(a) Remaining P cell population

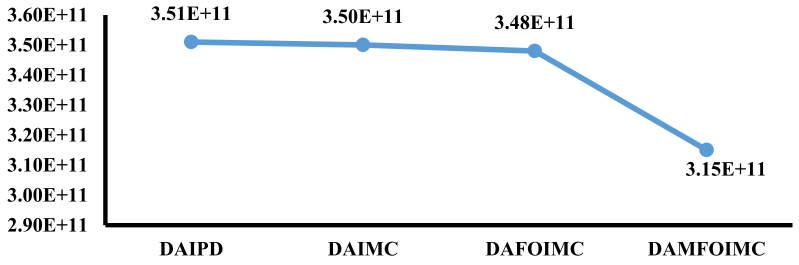

(b) Remaining Q cell population

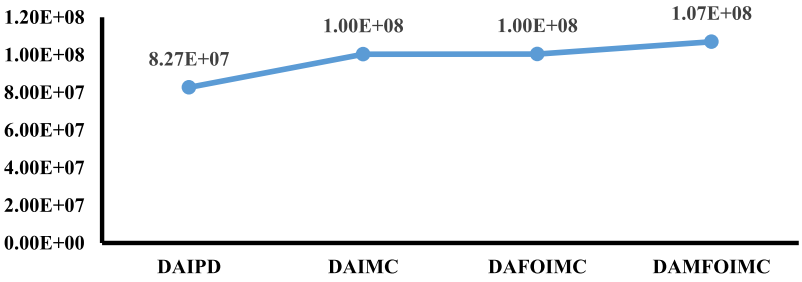

(c) Remaining Y cell population

Fig. 16. Comparison of designed controllers on the basis of remaining population of cells.

The gain parameters of the IPD controller and the filter coefficient in IMC controller were also tuned at $S_1 = 12.08$ by DA for the sake of making a fair comparison. The optimized values of the parameters are $K_P = 0.34$, $K_I = 0.162$, $K_D = 0.273$ and $\alpha = 0.72$. Fig. 14 shows the convergence curves for the IPD and IMC control schemes.

Changes in the set-point may completely change the behaviour of a process. Therefore, a set-point tracking analysis was carried out, considering three set-points. The drug concentration was changed from 12.08 mg/ml to 12.98 mg/ml, 12.98 mg/ml to 11.66 mg/ml at an interval of 28 days. The comparative analysis of the set-point tracking of the designed controllers is shown in Fig. 15(a). It can be seen from the results that DAMFOIMC reduces the overshoot and settling time significantly in comparison to other designed controllers. It can also be seen that the performances of DAIMC and DAFOIMC are almost similar. The corresponding variations in the number of P, Q, and Y cells are shown in Fig. 15 (b), (c) and (d) respectively. The comparison of the integral square error (ISE) and integral absolute error (IAE) for the entire time period is given in Table 9 along with the average toxicity values. It can be seen from the results that DAMFOIMC outperforms the other designed controllers, with the minimum average toxicity level.

Fig. 16 shows the comparison of designed controllers in terms of the remaining population of cells. The results show that the populations of remaining P and Q cells are smaller with the DAMFOIMC controller. The number of normal cells is larger with DAMFOIMC than with the other designed control strategies. Thus the patient is in a better state when the drug dose is determined using DAMFOIMC.

5.3. Robustness analysis for parametric uncertainty

A two-compartment cancer model has been used to estimate the optimum drug scheduling scheme. The preceding analysis was accomplished for the values of the parameters of the model given in Table 1. The values are considered to be fixed during the course of treatment. The values of the parameters of the mathematical model depend upon the physiological condition of the patient and tumor. The controller must be robust enough to provide adequate drug doses for changes in the values of the parameters of the model. Therefore, the parameter values of the proposed controller are the same as those given in Table 4. A robustness analysis of the designed controller was carried out to realize similar physiological and cancerous conditions of different patients. The analysis also considers minor changes in the starting time of treatment. These conditions may be modeled using ± 5% or ± 10% change in the model parameters a, m, β, μ and s_1. The closed loop control system was simulated for these changes and the results recorded are shown in Fig. 17. It can be seen from Fig. 17(a) that the number of P cells remains unchanged for uncertain model parameters. A similar trend is present in the reduction of the number of Q cells and Y cells as shown in Fig. 17(b) and (c) respectively. Table 10 shows the quantitative analysis of the proposed controller for model parametric uncertainty.

It can be seen from Table 10 that the proposed controller has a stable performance under parametric variations. Thus DAMFOIMC proves to be less sensitive to parametric uncertainty.

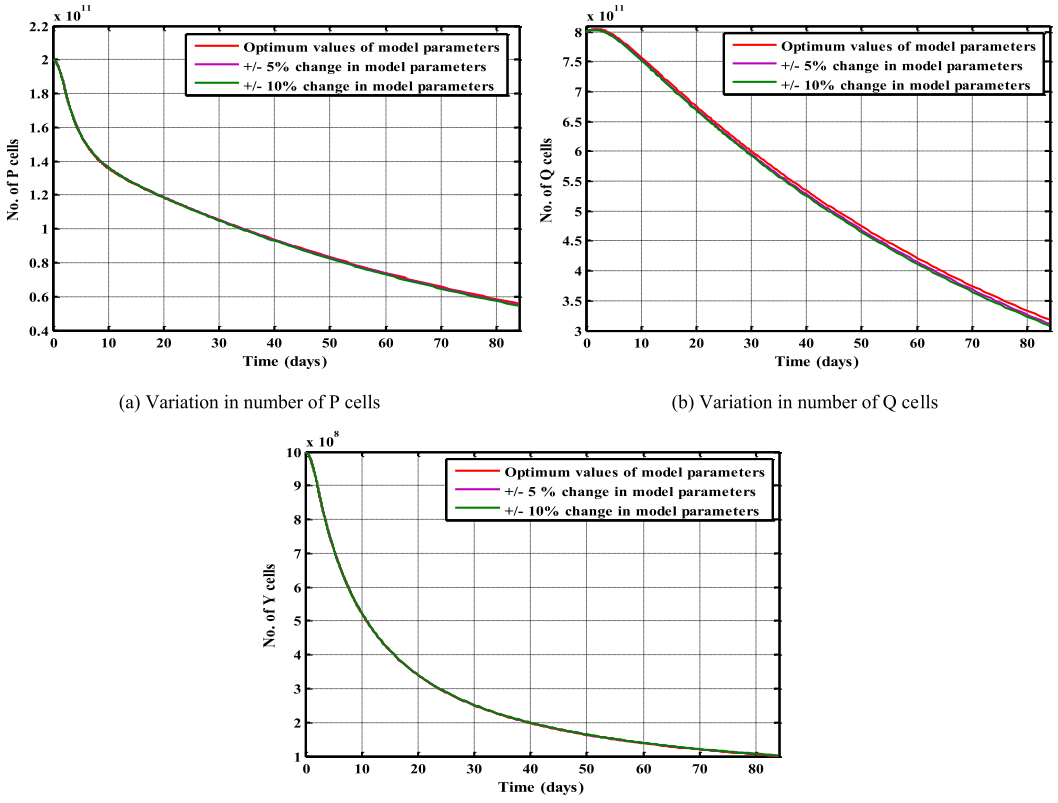

(a) Variation in number of P cells

(b) Variation in number of Q cells

(c). Variation in number of Y cells

Fig. 17. DAMFOIMC performance analysis for parametric uncertainty.

Table 10
Quantitative analysis of proposed controller for model parametric uncertainty.

Parameters	Reduction in P cells	Reduction in Q cells	Number of Y cells remaining	Maximum toxicity
Optimum values	72.1%	60.2%	$1.0089*10^8$	30.4
Parameter variation by ± 5%	72.4%	60.5%	$1.0191*10^8$	31.2
Parameter variation by ± 10%	72.7%	60.9%	$1.0243*10^8$	32.1

Table 11
Description of model parameters and initial values.

Variables	*Description*	*Values*
α	Growth speed of cancer cells	*1.5 x* 10^{-4} per *day*
μ	Elimination rate constant of drug toxicity	*0.4* per *day*
β	Threshold level of drug concentration	*10 drug unit*
γ	Biochemical character of drug	*0.27* per *day*
N(t)	Number of cancerous cells per unit time	$N(0) = 10^{10}$

Table 12
Optimized parameter values of designed controllers.

Controllers	K_P	K_I	K_D	η	α	K_{Pa}
DAIPD	0.36	0.164	0.269	–	–	–
DAIMC	–	–	–	–	0.782	–
DAFOIMC	–	–	–	0.75	–	–
DAMFOIMC	–	–	–	0.86	–	80

5.4. Case study 2

The performance of the proposed controller has also been tested on another cancer patient model. The chemotherapy model for cancer treatment developed by Martin [4,5] has been considered in this work.

The mathematical equations of the model are

$$\frac{dX(t)}{dt} = -\alpha X(t) + k(D(t) - \beta)H(D(t) - \beta) \tag{37}$$

$$H(D(t) - \beta) = \begin{Bmatrix} 1 & if\ D(t) \geq 0 \\ 0 & if\ D(t) \leq 0 \end{Bmatrix} \tag{38}$$

$$\frac{dD(t)}{dt} = u(t) - \gamma D(t),\ u(0) = 0 \tag{39}$$

$$\frac{dT(t)}{dt} = D(t) - \mu T(t) \tag{40}$$

The description of the parameters and initial values is given in Table 11 [4,5].

Initially, the FOIMC was designed by approximating the model as a FO plant model. Further, an MFOIMC was designed by following the previously discussed procedure. IPD and IMC controllers have also been developed for the model. The parameters of the designed controllers have been optimized using DA. The optimum parameter values for all the controllers are shown in Table 12.

The results obtained for drug concentration control using various controllers are shown in Fig. 18. The designed controllers have also been verified for positive and negative changes in the set-point while using the same controller parameters. The drug concentration is

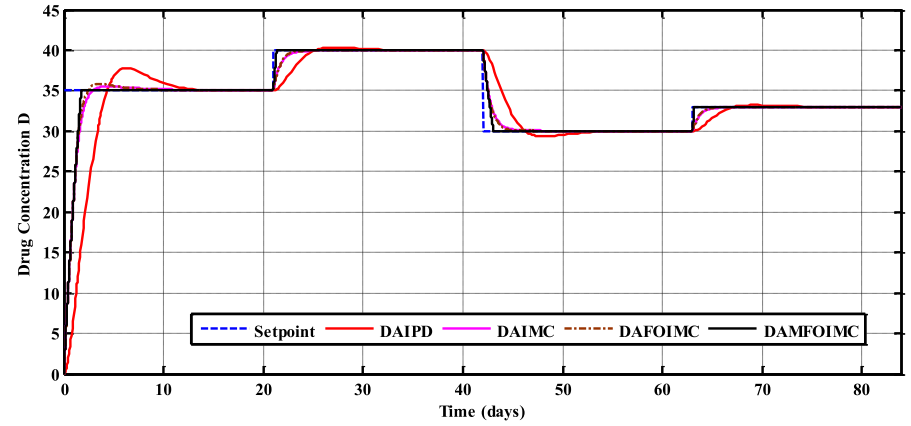

(a) Drug concentration D

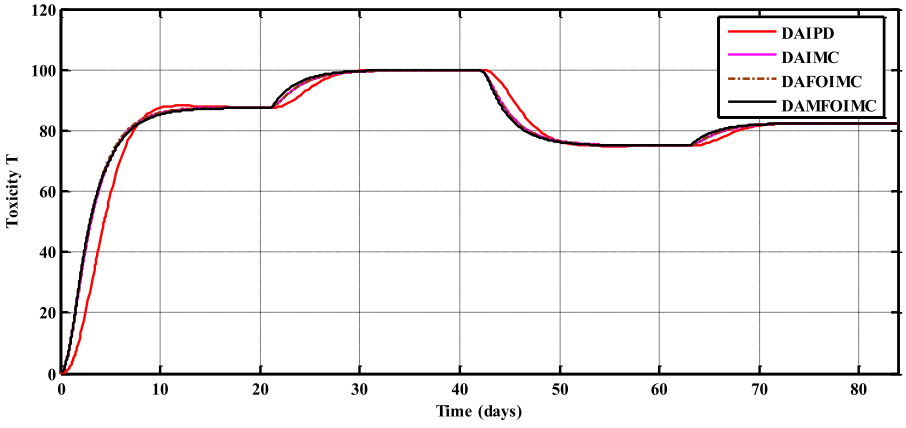

(b) Toxicity T

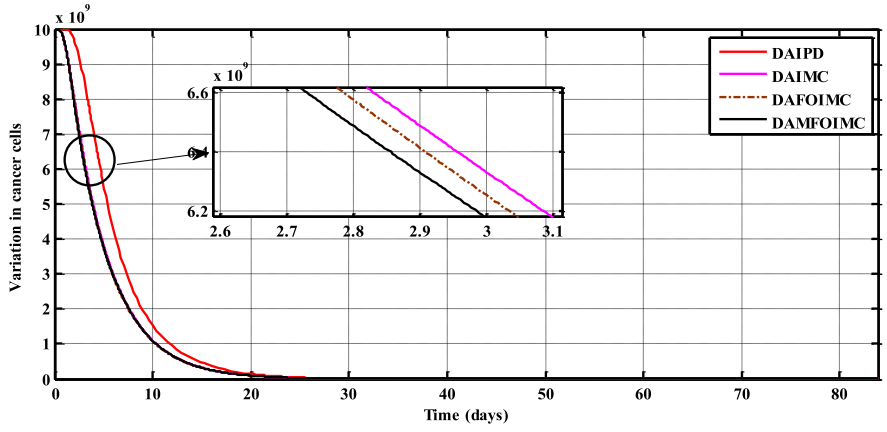

(c) Reduction in cancer cells

Fig. 18. Comparison of designed controllers for drug concentration control.

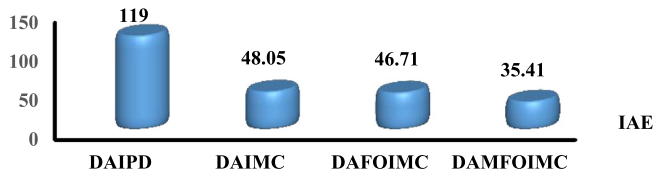

Fig. 19. IAE values for various designed controllers.

maintained at 35 mg/ml for the first 21 days. Then it is altered from 35 mg/ml to 40 mg/ml, 40 mg/ml to 30 mg/ml, and 30 mg/ml to 32 mg/ml at an interval of 21 days. It can be seen from Fig. 18(a) that DAMFOIMC improves the steady state and transient performance of the system by reducing the overshoot and settling time, in contrast to the other implemented controllers. Thus, the proposed controller is superior to the other controllers for regulating a servo problem. The corresponding variations in toxicity and number of cancer cells are shown in Fig. 18(b) and (c) respectively. The comparison of IAE shown in Fig. 19 also verifies the effectiveness of DAMFOIMC for drug concentration control. After the completion of the treatment period, the number of cancer cell remaining in case of DAMFOIMC is 41.24, which is less than for the other designed controllers.

6. Discussion

A fusion of IMC and the fractional calculus (MFOIMC) has been

suggested for closed loop drug concentration control during chemotherapy. The performance of the proposed controller has been compared with that of FOIMC, Integer order IMC, and IPD controllers. After a rigorous performance comparison with GA, SA, KH and PSO, the DA has been selected to set the optimum values of the controller parameters. It has been seen that DA takes fewer NFEs to reach its optimum values, and with lesser fitness values. The performance of the designed controllers was tested on two different mathematical models. The models and parameters under consideration were quantitatively derived by Martin and his colleagues [3–5,12] for lung and breast cancer patients.

The eradication of cancer cells depends upon the drug dose injected into the patient at the tumor site. A high drug dose kills cancer cells at a faster rate, but on the other hand it increases the toxicity level in the patient's body. If the level of toxicity increases beyond a certain threshold, the population of normal cell decreases very fast, which risks the patient's life. Thus a higher drug dose directly influences the survival of the patient. For this reason, the output of the controller is limited to 7 mg-day/ml (Figs. 10a and 11a) with the help of a limiter. Initially the number of cancerous cells is larger and the effect of drug is subject to a time delay. Therefore, the drug dose evaluated by the control algorithm is higher than the threshold. However, the limiter keeps it in the permissible limits and a constant drug dose is maintained initially for some days (Fig. 10). This allows the maximum possible cancerous cell killing and later on the drug dose settles down according to the response of the patient's body.

The simulation results showed that DAMFOIMC schedules the drug dose in such a way that the drug concentration reaches the set-point in the minimum time in comparison to the other designed controllers. The proposed control scheme reduces significantly the number of cancerous cells (P and Q cells). Most prominently, the maximum value of toxicity during the course of treatment is much lower than its maximum allowable value as given in Equation (7) and suggested in the literature [11,12,15]. Further the robustness to parametric uncertainty of the proposed drug schedule scheme was investigated. It is evident from the analysis that in spite of model uncertainties, the reduction in cancerous cells in the presence of model parametric uncertainty is nearly identical to that without such uncertainty. It is essential to note that DAMFOIMC is exceptionally stable and effective regardless of variations in model parameters. Thus DAMFOIMC provides an effective solution to drug concentration control at tumor site during chemotherapy.

The mathematical model considered for this work is semi-rigorous, as it does not include the constraints of protein binding for drug transportation. The performance of the proposed control scheme could also be tested on rigorous cancer patient model which includes all physiological and biological conditions of patient. Previous studies have suggested that findings based on mathematical models can be tested clinically with encouraging results [36]. However mathematical models possess few limitations:

- ➢ Lack of resolution regarding efficacy of mathematical model based study versus real time treatment.
- ➢ The predictive capability of a mathematical model depends upon its accuracy, the biological assumptions, and the quality of the data.
- ➢ Due to the advances in technology, more complex insights into tumor biology are emerging, such as single cell genetics, epigenetic heterogeneity, microenvironments, etc. All these features need to be incorporated into mathematical models to bridge the gap between the mathematical model and the cancer patient.

7. Conclusion

In this paper a dragonfly algorithm (DA) tuned modified fractional order internal model control (DAMFOIMC) scheme has been proposed for the effective and accurate control of the drug concentration at the tumor site during chemotherapy in minimal time, with optimal drug doses. Initially, an FOIMC controller was designed and implemented for the control of the drug concentration, which was then modified by introducing an extra feedback loop with a proportional transfer function, leading to the MFOIMC. The design parameters of both controllers were optimized using the DA optimization technique. The drug concentration provided by DAMFOIMC reaches its reference point in the minimum time with the minimum overshoot and settling time, compared to DAFOIMC. Further, the performance of DAMFOIMC for different set-points has been compared with DA tuned versions of IPD, internal model control, and fractional order internal model controllers. It has been shown that the percentage of killing of P and Q cells with minimum toxicity is higher with DAMFOIMC than with these other controllers. The robustness of the proposed controller has also been analysed under parametric uncertainties. It is concluded that DAMFOIMC for drug concentration control is robust, stable, efficient and simple in structure, with only two design parameters. In the future, the proposed scheme may be applied to real time data.

Conflict of interest

It is hereby announced that there is no conflict of interest between authors and to anybody else

References

[1] http://www.who.int/topics/cancer/en/.
[2] http://www.icmr.nic.in/icmrsql/archive/2016/7.pdf.
[3] P. Dua, V. Dua, N. Pistikopoulos, Optimal delivery of chemotherapeutic agents in cancer, Comput. Chem. Eng. 32 (2008) 99–107.
[4] R.B. Martin, Optimal Control of Drug Administration in Cancer Chemotherapy, Ph.D. thesis School of Computer & Information Sciences, University of Western Australia, Perth, Australia, 1991.
[5] R.B. Martin, Optimal control drug scheduling of cancer chemotherapy, Automatica 28 (1992) 1113–1123.
[6] B. Bojkov, R. Hansel, R. Luus, Application of direct search optimization to optimal control problems, Hung. J. Ind. Chem. 21 (1993) 177–185.
[7] K. Tan, E.F. Khor, J. Cai, C.M. Heng, T.H. Lee, Automating the drug scheduling of cancer chemotherapy via: evolutionary computation, Artif. Intell. Med. 1 (2002) 908–913.
[8] Y. Liang, K.S. Leung, T.S.K. Mok, A novel evolutionary drug scheduling model in cancer chemotherapy, IEEE Trans. Inf. Technol. Biomed. 10 (2006) 237–245.
[9] S. Tes, Y. Liang, K.S. Leung, K. Lee, T.S. Mok, A memetic algorithm for multiple-drug cancer chemotherapy scheduling optimization, IEEE Trans. Syst.ManCybern. 37 (2007) 84–91.
[10] Y. Liang, K. Leung, T. Mok, Evolutionary drug scheduling models with different toxicity metabolism in cancer chemotherapy, Appl. Soft Comput. 8 (2008) 140–149.
[11] S. Algoul, M.S. Alam, M.A. Hossain, M.A.A. Majumder, Multi-objective optimal chemotherapy control model for cancer treatment, Med. Biol. Eng. Comput. 49 (2011) 51–65.
[12] M.S. Alam, M.A. Hossain, S. Algoul, M.A.A. Majumader, M.A. Al-Mamun, G. Sexton, R. Phillips, Multi-objective multi-drug scheduling schemes for cell cycle specific cancer treatment, Comput. Chem. Eng. 58 (2013) 14–32.
[13] H. Moradi, G. Vossoughi, H. Salarieh, Optimal robust control of drug delivery in cancer chemotherapy: a comparison between three control approaches, Comput. Biol. Med. 112 (2013) 69–82.
[14] L. Kovácsa, A. Szeles, J. Sápi, A.D. Dániel, Harmati I. Rudas, Z. Sápi, Model-based angiogenic inhibition of tumor growth using modern robust control method, Comput. Methods Progr. Biomed. 114 (2014) 98–110.
[15] S. Khadraoui, F. Harrou, H.N. Nounou, N. Nounou, A. Datta, P. Bhattacharyya, A measurement-based control design approach for efficient cancer chemotherapy, Inf. Sci. 333 (2016) 108–125.
[16] Vivek Pandey, Pachauri Nikhil, Rani Asha, Vijander Singh, Optimal ISA-PID-based drug concentration control in cancer chemotherapy, book chapter in, Advances in Intelligent Systems and Computing, 2018, pp. 165–171.
[17] Q.B. Jin, Q. Liu, Analytical IMC-PID design in terms of performance/robustness tradeoff for integrating processes: from 2-Dof to 1-Dof, J. Process Control 24 (2014) 22–32.
[18] D.B. Santosh Kumar, R. Padma Sree, Tuning of IMC based PID controllers for integrating systems with time delay, ISA (Instrum. Soc. Am.) Trans. 63 (2016) 242–255.
[19] T. Liu, F. Gao, Enhanced IMC design of load disturbance rejection for integrating and unstable processes with slow dynamics, ISA (Instrum. Soc. Am.) Trans. 50 (2011) 239–248.
[20] A.K. Yadav, P. Gaur, Intelligent modified internal model control for speed control of nonlinear uncertain heavy duty vehicles, ISA (Instrum. Soc. Am.) Trans. 56 (2015) 288–298.
[21] U. Saggaf, I. Mehedi, M. Bettayeb, R. Mansouri, Fractional-order controller design for a heat flow process, J. Syst. Control Eng. 7 (2016) 1–12.

[22] S. Mirjalili, Dragonfly algorithm: a new meta-heuristic optimization technique for solving single-objective discrete and multi-objective problems, Neural Comput. Appl. 27 (2015) 1–21.
[23] D. Tiwari, N. Pachauri, A. Rani, V. Singh, Fractional order PID (FOPID) controller based temperature control of bioreactor, Int. Conf. Electr. Electron. Optim. Tech. (2016) 2968–2973.
[24] G. Raman, G. Raman, C. Manickam, S.I. Ganesan, Dragonfly algorithm based global maximum power point tracker for photovoltaic systems, Adv. Swarm Intell. 9712 (2016) 211–219.
[25] M. Hamdy, A.T. Nguyen, J.L.M. Hensen, A performance comparison of multi-objective optimization algorithms for solving nearly-zero-energy-building design problems, Energy Build. 121 (2016) 57–71.
[26] V. Suresh, S. Sreejith, Generation dispatch of combined solar thermal systems using dragonfly algorithm, Computing 99 (2017) 59–80.
[27] C. Sawyers, Targeted cancer therapy, Nature 432 (2004) 294–297.
[28] Vijay Mohan, Himanshu Chhabra, Asha Rani, Vijander Singh, An expert 2DOF fractional order fuzzy PID controller for Nonlinear systems, Neural Comput. Appl. (2018) 1–18.
[29] Nikhil Pachauri, Vijander Singh, Asha Rani, Two degrees-of-freedom fractional-order proportional–integral– derivative- based temperature control of fermentation process, J. Dyn. Syst. Meas. Control 140 (7) (2018) 1–10.
[30] N. Pachauri, A. Rani, V. Singh, Two degree of freedom PID based inferential control of continuous bioreactor for ethanol production, ISA Trans. 68 (2017) 235–250.
[31] J. Shrager, J.M. Tenenbaum, Rapid learning for precision oncology, Nat. Rev. Clin. Oncol. 11 (2014) 109–118.
[32] M.M. Gottesman, T. Fojo, S.E. Bates, Multidrug resistance in cancer: role of ATP-dependent transporters, Nat. Rev. Canc. 2 (2002) 48–58.
[33] C. Holohan, S. Van Schaeybroeck, D.B. Longley, P.G. Johnston, Cancer drug resistance: an evolving paradigm, Nat. Rev. Canc. (2013) 714–726.
[34] W. Hryniuk, Dosage parameters in chemotherapy of breast cancer, Breast Dis. 14 (2001) 21–30.
[35] D.E. Lake, C.A. Hudis, High-dose chemotherapy in breast cancer, Drugs 64 (2004) 1851–1860.
[36] F. Michor, K. Beal, Improving cancer treatment via mathematical modeling: surmounting the challenges is worth the effort, Cell 163 (2015) 1059–1063.
[37] U. Ledzewicz, U. Schattler, Marriott J Piecewise constant suboptimal controls for a system describing tumor growth under angiogenic treatment, 18th IEEE International Conference on Control Applications, 2009, pp. 77–82.
[38] H. Ruotsalainen, E. Boman, K. Miettinen, J. Tervo, Nonlinear interactive multi-objective optimization method for radiotherapy treatment planning with Boltzmann transport equation, Contemp Eng Sci. 2 (2009) 391–422.
[39] N. Pachauri, A. Rani, V. Singh, Bioreactor temperature control using modified fractional order IMC-PID for ethanol production, Chem. Eng. Res. Des. 122 (2017) 97–112.
[40] D. Li, L. Liu, Q. Jin, K. Hirasawa, Maximum sensitivity based fractional IMC–PID controller design for non-integer order system with time delay, J. Process Control 31 (2015) 17–29.
[42] M.T. Kakhki, M. Haeri, M.S. Tavazoei, Simple fractional order model structures and their applications in control system design, Eur. J. Control 6 (2010) 680–694.
[43] M.T. Kakhki, M. Haeri, Fractional order model reduction approach based on retention of the dominant dynamics: application in IMC based tuning of FOPI and FOPID controllers, ISA (Instrum. Soc. Am.) Trans. 50 (2011) 432–442.
[44] T. Vinopraba, N. Sivakumaran, S. Narayanan, T.K. Radhakrishnan, Design of internal model control based fractional order PID controller, J. Control Theor. Appl. 10 (3) (2012) 297–302, https://doi.org/10.1007/s11768-012-1044-4.
[45] Mingjie Li, Ping Zhou, Zhicheng Zhao, Jinggang Zhang, Two-degree-of-freedom fractional order-PID controllers design for fractional order processes with dead-time, ISA (Instrum. Soc. Am.) Trans. 61 (2016) 147–154.
[46] Y.Q. Chen, Impulse Response Invariant Discretization of Fractional Order Integrators/differentiators Is to Compute a Discrete- Time Finite Dimensional (Z) Transfer Function to Approximates^r with R a Real Number URL, www.mathworks.com.
[47] D.H. Wolpert, W.G. Macready, No free lunch theorems for optimization, IEEE Trans. Evol. Comput. 1 (1997) 67–82.
[48] M. Jain, V. Singh, A. Rani, A Novel Nature-Inspired Algorithm for Optimization: Squirrel Search Algorithm, Swarm Evol. Comput. 44 (2019) 148–175.
[49] A.H. Gandomia, A.H. Alavib, Krill herd: a new bio-inspired optimization algorithm", Commun. Nonlinear Sci. Numer. Simul. 17 (12) (2012) 4831–4845.
[50] S. Choudhary, "Stability and performance analysis of fractional order control systems", WSEAS Trans. Syst. Control, 9.
[51] J.C. Panetta, J. Adam, A mathematical model of cycle-specific chemotherapy, Math. Comput. Model. 22 (1995) 67–82.
[52] B. Panjwani, V. Mohan, A.Rani, V. Singh, "Optimal drug scheduling for cancer chemotherapy using two degree of freedom fractional order PID scheme", J. Intell. Fuzzy Syst., 36 (3), 2273-2284.